

## Scattering from an infinite dielectric cylinder embedded into another

This article has been downloaded from IOPscience. Please scroll down to see the full text article.

1979 J. Phys. A: Math. Gen. 12 825

(<http://iopscience.iop.org/0305-4470/12/6/011>)

View [the table of contents for this issue](#), or go to the [journal homepage](#) for more

### Download details:

IP Address: 129.252.86.83

The article was downloaded on 01/06/2010 at 16:06

Please note that [terms and conditions apply](#).

# Scattering from an infinite dielectric cylinder embedded into another

N K Uzunoglu and J G Fikioris

Chair of Wireless and Long Distance Communication, Department of Electrical Engineering, National Technical University of Athens, Athens 147, Greece

Received 10 July 1978, in final form 9 November 1978

**Abstract.** In this work the scattering from an infinite dielectric cylinder embedded into another cylinder is considered. In the case of an eccentric circular cylinder the problem is solved using the classical separation of variables techniques combined with related translational addition theorems. When the difference in the indices of refraction of the cylinders is small a perturbation series is developed up to second order. For non-circular arbitrary inhomogeneities, an integral equation method is developed by employing the homogeneous scatterer Green function. Numerical results are computed for circular cylindrical inhomogeneities; the convergence of the perturbation series and the properties of the scattered field are discussed.

## 1. Introduction

Scattering from complex bodies is often used for detecting possible internal inhomogeneities and non-symmetries. By observing the field scattered by a body on which radiation is impinging it is possible to obtain information about its internal structure. Investigation of cells (Wyatt and Phillips 1972) and of biological bodies (Guru and Chen 1976), remote sensing techniques (Latimer and Pyle 1972) and detection of imperfections inside optical waveguides and lenses and straightforward examples.

The literature on scattering from inhomogeneous scatterers is mostly concentrated on scatterers with radially stratified dielectric distributions (Kerker 1969). In this work the scattering from arbitrary infinitely long dielectric cylinders embedded into other such cylinders is considered (see figure 1). With  $n'$  and  $n$  denoting the corresponding indices of refraction of the cylinders a perturbation series in powers of  $(n' - n)$  is developed that allows quick and simple evaluation of the external and internal fields for small values of  $(n' - n)$ . In particular, the case of an eccentric circular inhomogeneity (see figure 2) is solved by employing separation of variables together with related translational addition theorems for cylindrical wavefunctions. In this way satisfaction of the boundary conditions at both interfaces leads to appropriate sets of linear equations for the determination of the expansion coefficients. Then a perturbation series in powers of the difference  $(n' - n)$  is developed which allows an analytic solution to second order in  $(n' - n)$ . The series can be easily extended to include higher-order terms.

For non-circular inhomogeneities, i.e. for an arbitrarily shaped imperfection as shown in figure 1, the problem is formulated by the Green function method. For

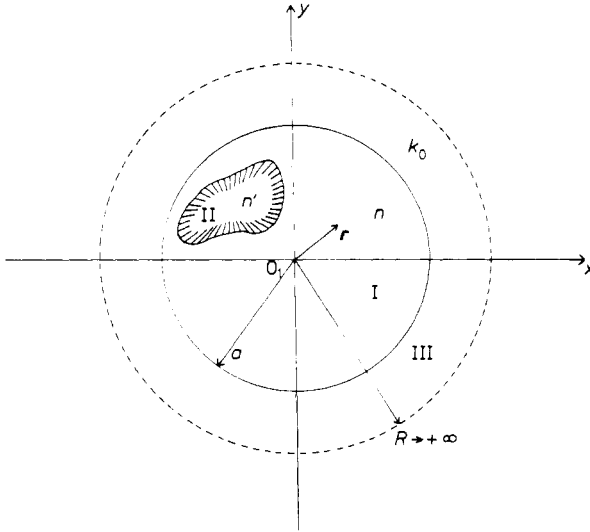


**Figure 1.** Infinitely long cylinder geometry with arbitrarily shaped inhomogeneity.

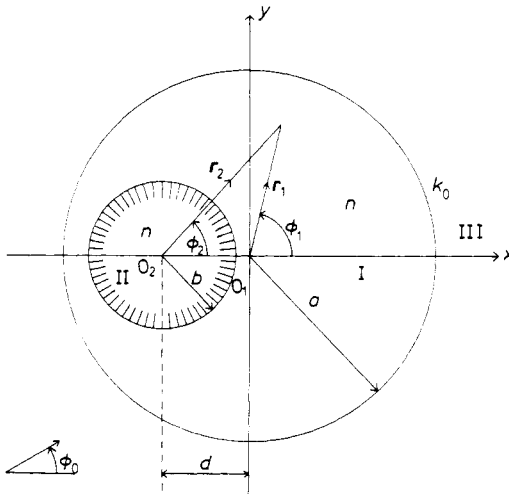


**Figure 2.** Circular inhomogeneity inside a circular infinitely long dielectric cylinder.

three-dimensional scatterers—such as spheres with internal inhomogeneities—the problem has also been investigated and will be published elsewhere.

Numerical results have been computed for several cases; the convergence of the perturbation series and the scattering properties of such complex scatterers is also discussed later in this paper.

## 2. Eccentric circular inhomogeneity

The geometry of the problem is defined in figure 2, where  $a$ ,  $b$  are the outer and inner cylinder radii, while the inter centre distance of the cylinders is represented by  $d$ . The

refractive indices of media I and II are  $n$  and  $n'$  respectively. The inner cylinder centre is assumed always to be on the negative  $x$  axis. The wavenumber of free space, region III, is denoted by  $k_0$ . Both  $E$ - and  $H$ -wave polarisations will be considered at the same time. The incident wave impinging normally on the  $z$  axis has the form

$$\begin{aligned} E_0(x, y) &= \hat{z} \exp(ik_0r_1 \cos(\phi_1 - \phi_0)) && (E \text{ wave}) && (r_1 \geq a) \\ H_0(x, y) &= \hat{z} \exp(ik_0r_1 \cos(\phi_1 - \phi_0)) && (H \text{ wave}) \end{aligned} \quad (1)$$

where  $r_1, \phi_1$  are the polar coordinates and  $\phi_0$  is the direction of propagation of the incident wave. The assumed time dependence is  $\exp(-i\omega t)$ .

Since the fields are independent of the  $z$  coordinate, scalar potentials can be used to describe them. The incident wave can then be expressed as

$$\Psi_0^{E,H} = \exp(ik_0r_1 \cos(\phi_1 - \phi_0)) = \sum_{m=-\infty}^{+\infty} i^m J_m(k_0r_1) \exp[im(\phi_1 - \phi_0)]. \quad (2)$$

For the regions I and II of figure 2, the fields can be expanded into cylindrical wavefunctions with respect to the origin  $O_2$  as follows:

$$\Psi_I^{E,H} = \sum_{m=-\infty}^{+\infty} (a_m^{E,H} J_m(nk_0r_2) + b_m^{E,H} Y_m(nk_0r_2)) \exp(im\phi_2) \quad (r_2 \geq b) \quad (3)$$

$$\Psi_{II}^{E,H} = \sum_{m=-\infty}^{+\infty} c_m^{E,H} J_m(n'k_0r_2) \exp(im\phi_2) \quad (r_2 \leq b) \quad (4)$$

where  $r_2, \phi_2$  are the cylindrical coordinates with respect to the origin  $O_2$  and  $J_m$  and  $Y_m$  are the usual cylindrical Bessel and Neuman functions. Employing the boundary conditions at  $r_2 = b$

$$\Psi_I^E = \Psi_{II}^E \quad \partial\Psi_I^E/\partial r_2 = \partial\Psi_{II}^E/\partial r_2 \quad (5)$$

and

$$\Psi_I^H = \Psi_{II}^H \quad n^{-2} \partial\Psi_I^H/\partial r_2 = n'^{-2} \partial\Psi_{II}^H/\partial r_2 \quad (6)$$

and using the identity  $z'_n(x) = (n/x)z_n(x) - z_{n+1}(x)$  for the Bessel functions the following equations are obtained:

$$\frac{b_m^E}{\alpha_m^E} = \frac{xJ_{m+1}(x)J_m(x') - x'J_{m+1}(x')J_m(x)}{x'J_{m+1}(x')Y_m(x) - xJ_m(x')Y_{m+1}(x)} = F_m^E(x', x) \quad (7)$$

and

$$\frac{b_m^H}{\alpha_m^H} = \frac{xJ_m(x)J'_m(x') - x'J'_m(x)J_m(x')}{x'J'_m(x')Y'_m(x) - xJ'_m(x')Y_m(x)} = F_m^H(x', x) \quad (8)$$

where  $x = nk_0b, x' = n'k_0b$ .

The translational addition theorems for cylindrical wavefunctions transform the expansion of  $\Psi_I^{E,H}$  around the origin  $O_2$  to an expansion around the origin  $O_1$ . Assuming that the point  $(r_1, \phi_1)$  is always outside the circle with diameter  $O_1O_2$  the addition theorem from Stratton (1941) and appendix 1 has the form

$$Z_m(nk_0r_2) \exp(im\phi_2) = \sum_{\kappa=-\infty}^{+\infty} J_{m-\kappa}(t) Z_\kappa(nk_0r_1) \exp(i\kappa\phi_1) \quad (9)$$

where  $r_1 > |d \cos \phi_1|$ ,  $Z_m(x) = \alpha J_m(x) + b Y_m(x)$  is the general Bessel function and

$t = nk_0d$ . Substituting equation (9) into equation (3) the field with respect to the origin  $O_1$  is expressed as

$$\begin{aligned} \Psi_1^{E,H} &= \sum_{m=-\infty}^{+\infty} \left( \alpha_m^{E,H} \sum_{K=-\infty}^{+\infty} J_{m-K}(t) J_K(nk_0r_1) \exp(iK\phi_1) + b_m^{E,H} \right. \\ &\quad \times \left. \sum_{K=-\infty}^{+\infty} J_{m-K}(t) Y_K(nk_0r_1) \exp(iK\phi_1) \right) \\ &= \sum_{m=-\infty}^{+\infty} (A_m^{E,H} J_m(k_0nr_1) + B_m^{E,H} Y_m(k_0nr_1)) \exp(im\phi_1) \end{aligned} \quad (10)$$

where a redefinition of indices has been used and the new coefficients are given as

$$\begin{aligned} A_m^{E,H} &= \sum_{K=-\infty}^{+\infty} J_{K-m}(t) \alpha_K^{E,H} \\ B_m^{E,H} &= \sum_{K=-\infty}^{+\infty} J_{K-m}(t) b_K^{E,H}. \end{aligned} \quad (11)$$

Also, the expansion of equation (10) can be transformed back with respect to the origin  $O_2$ , again using the addition theorem. In a way analogous to the previous procedure we can find the following relations:

$$\begin{aligned} \alpha_m^{E,H} &= \sum_{K=-\infty}^{+\infty} J_{m-K}(t) A_K^{E,H} \\ b_m^{E,H} &= \sum_{K=-\infty}^{+\infty} J_{m-K}(t) B_K^{E,H}. \end{aligned} \quad (12)$$

The scattered field outside the main scatterer (i.e.  $r_1 > a$ ) can be expanded in terms of cylindrical wavefunctions as

$$\Psi_S^{E,H} = \sum_{m=-\infty}^{+\infty} d_m^{E,H} H_m^{(1)}(k_0r_1) \exp(im\phi_1). \quad (13)$$

Expanding the incident plane waves of equation (1) in terms of cylindrical wavefunctions as shown in equation (2), substituting equations (13) and (10) into the boundary conditions at  $r_1 = a$ ,

$$\Psi_1^E = \Psi_0^E + \Psi_S^E \quad \partial\Psi_1^E/\partial r_1 = (\partial\Psi_0^E/\partial r_1) + (\partial\Psi_S^E/\partial r_1) \quad (14)$$

and

$$\Psi_1^H = \Psi_0^H + \Psi_S^H \quad n^{-2} \partial\Psi_1^H/\partial r_1 = (\partial\Psi_0^H/\partial r_1) + (\partial\Psi_S^H/\partial r_1) \quad (15)$$

the following equations are obtained:

$$A_m^{E,H} J_m(y) + B_m^{E,H} Y_m(y) = i^m J_m(v) \exp(-im\phi_0) + d_m^{E,H} H_m(v) \quad (16)$$

$$A_m^E y J'_m(y) + B_m^E y Y'_m(y) = i^m v J'_m(v) \exp(-im\phi_0) + d_m^E v H'_m(v) \quad (17)$$

$$A_m^H v J'_m(y) + B_m^H v Y'_m(y) = i^m y J'_m(v) \exp(-im\phi_0) + d_m^H y H'_m(v) \quad (18)$$

where  $y = nk_0a$ ,  $v = k_0a$ .

By eliminating the scattering coefficients  $d_m^E$ ,  $d_m^H$  from equations (16), (17) and (18) and by using equations (7), (8), (11) and (12), an infinite set of equations is obtained as

$$A_m^{E,H} = 2i^{m+1} \exp(-im\phi_0) P_m^{E,H}(y, v) - D_m^{E,H}(y, v) \sum_K J_{K-m}(t) F_K^{E,H}(x', x) \sum_S A_S^{E,H} J_{K-S}(t) \quad (19)$$

where

$$D_m^E(y, v) = \frac{yY_{m+1}(y)H_m(v) - Y_m(y)H_{m+1}(v)v}{yH_m(v)J_{m+1}(y) - J_m(y)H_{m+1}(v)v} \tag{20}$$

$$D_m^H(y, v) = \frac{yY_m(y)H'_m(v) - Y'_m(y)H_m(v)v}{yJ_m(y)H'_m(v) - J'_m(y)H_m(v)v}$$

$$P_m^E(y, v) = \frac{1}{\pi(yH_m(v)J_{m+1}(y) - J_m(y)H_{m+1}(v)v)} \tag{21}$$

$$P_m^H(y, v) = \frac{y}{\pi v(yJ_m(y)H'_m(v) - vJ'_m(y)H_m(v))}$$

The infinite set of equations (19), being the result of what is sometimes called in the literature a mode-matching technique (Mittra and Lee 1971), can be solved directly numerically by truncating the summations in order to obtain a matrix equation (Harrington 1968, Mittra 1973). However, whenever  $(x' - x)$  is small analytical procedure can be developed. Observing from equations (7) and (8) that

$$F_m^{E,H}(x', x)|_{x'=x} = 0$$

the following Taylor expansion can be written:

$$F_m^{E,H}(x', x) = (x' - x)F_m^{E,H}(1) + (x' - x)^2 A_m^{E,H}(2) + \dots \tag{22}$$

The expressions for  $F_m^{E,H}(1)$  and  $F_m^{E,H}(2)$  are given in appendix 2.

Assuming also an analytic expansion of the form

$$A_m^{E,H} = A_m^{E,H}(0) + (x' - x)A_m^{E,H}(1) + (x' - x)^2 A_m^{E,H}(2) + \dots \tag{23}$$

and substituting equations (22) and (23) into (19) yields the following expressions for the perturbation coefficients:

$$A_m^{E,H}(0) = 2i^{m+1} \exp(-im\phi_0) P_m^{E,H}(y, v) \tag{24}$$

$$A_m^{E,H}(1) = -D_m^{E,H}(y, v) \sum_{K=-\infty}^{+\infty} J_{K-m}(t) F_K^{E,H}(1) \sum_{S=-\infty}^{+\infty} A_S^{E,H}(0) J_{K-S}(t) \tag{25}$$

$$\begin{aligned} A_m^{E,H}(2) = & -D_m^{E,H}(y, v) \sum_{K=-\infty}^{+\infty} J_{K-m}(t) F_K^{E,H}(1) \sum_{S=-\infty}^{+\infty} A_S^{E,H}(1) J_{K-S}(t) \\ & + \sum_{K=-\infty}^{+\infty} J_{K-m}(t) F_K^{E,H}(2) \sum_{S=-\infty}^{+\infty} A_S^{E,H}(0) J_{K-S}(t). \end{aligned} \tag{26}$$

Obviously this perturbation can be continued indefinitely at the cost, however, of increasing the complexity of the coefficients  $F_K^{E,H}(n)$ . After determining the set of coefficients  $A_m^{E,H}$  we can eliminate the coefficients  $B_m^{E,H}$  from equations (16), (17) and (18) and obtain simple expressions for the scattered field coefficients  $d_m^{E,H}$  in terms of  $A_m^{E,H}$ . These are then used to find the scattered field

$$\Psi_S^{E,H} = (2/\pi k_0 r_1)^{1/2} \exp(ik_0 r_1 - \frac{1}{4}i\pi) G^{E,H}(\phi_1) \tag{27}$$

in terms of the scattering amplitude  $G^{E,H}(\phi_1)$ , which is defined as

$$G^{E,H}(\phi_1) = \sum_{m=-\infty}^{+\infty} d_m^{E,H} i^{-m} \exp(im\phi_1). \tag{28}$$

Numerical results for eccentric circular inhomogeneities are presented in § 4.

### 3. Arbitrarily shaped inhomogeneities; the Green function method

For the case of an arbitrarily shaped inhomogeneity the method of separation of variables cannot be used. Since the boundary conditions for  $r_1 = a$  are regular a Green function method is suggested as follows. Only the  $E$ -wave polarisation will be considered. Analogous results hold for the  $H$ -wave polarisation.

In order to determine the Green function for the homogeneous cylinder ( $|r| \leq a$ ) (see figure 1), we use the method developed by Sommerfeld (1964). The Green function is defined as the response field to a unit source excitation. The primary field from a unit excitation at  $r'$  is given as

$$G_0(\mathbf{r}, \mathbf{r}') = \frac{1}{4i} H_0(k_0|\mathbf{r} - \mathbf{r}'|) = \frac{1}{4i} \sum_{m=-\infty}^{+\infty} J_m(nk_0r_{<}) H_m(nk_0r_{>}) \exp[im(\phi - \phi')] \tag{29}$$

where  $r_{\lessgtr} = \begin{matrix} \min \\ \max \end{matrix} (r, r')$  and  $r' < a$ .

The induced field inside the cylinder can be expanded into a sum of cylindrical wavefunctions as

$$G_1(\mathbf{r}, \mathbf{r}') = \sum_{m=-\infty}^{+\infty} f_m J_m(nk_0r) \exp[im(\phi - \phi')] \tag{30}$$

and the field outside can be written as

$$G_2(\mathbf{r}, \mathbf{r}') = \sum_{m=-\infty}^{+\infty} g_m H_m^{(1)}(k_0r) \exp[im(\phi - \phi')]. \tag{31}$$

The Green function defined as the total field of the unit excitation is given as

$$\begin{aligned} G(\mathbf{r}, \mathbf{r}') &= G_0(\mathbf{r}, \mathbf{r}') + G_1(\mathbf{r}, \mathbf{r}') && \text{for } |\mathbf{r}| \leq a \\ &= G_2(\mathbf{r}, \mathbf{r}') && \text{for } |\mathbf{r}| \geq a. \end{aligned} \tag{32}$$

The unknown coefficients  $f_m, g_m$  are determined by using the boundary conditions

$$G_0 + G_1 = G_2 \quad (\partial G_0 / \partial r) + (\partial G_1 / \partial r) = \partial G_2 / \partial r \quad \text{for } |\mathbf{r}| = a \tag{33}$$

and after some lengthy algebra the Green function is obtained in the form:

$$G(\mathbf{r}, \mathbf{r}') = \frac{1}{4} \sum_{m=-\infty}^{+\infty} \exp[im(\phi - \phi')] T_m(\mathbf{r}, \mathbf{r}') \tag{34}$$

where

$$\begin{aligned} T_m(\mathbf{r}, \mathbf{r}') &= J_m(nk_0r) J_m(nk_0r') D_m^E(y, v) - J_m(nk_0r_{<}) Y_m(nk_0r_{>}) && \text{for } r \leq a \\ &= H_m(k_0r) J_m(nk_0r') P_m^E(y, v) && \text{for } r \geq a \end{aligned} \tag{35}$$

and  $r' < a$ .

Using the standard Green theorem and the theory of Green functions (Morse and Feshbach 1953) we obtain the relation

$$\Psi^E(\mathbf{r}) = \Phi_0(\mathbf{r}) + k_0^2(n'^2 - n^2) \int_{II} d\mathbf{r}' G(\mathbf{r}, \mathbf{r}') \Psi^E(\mathbf{r}') \tag{36}$$

where

$$\Phi_0(\mathbf{r}) = \Psi_0^E(\mathbf{r}) + k_0^2(n^2 - 1) \int_{I+II} G(\mathbf{r}, \mathbf{r}') \Psi_0^E(\mathbf{r}') d\mathbf{r}' \tag{37}$$

Note that if both  $\mathbf{r}$  and  $\mathbf{r}'$  are restricted inside region II in equation (36) we obtain an integral equation for the field inside the region of inhomogeneity. If this is determined from the integral equation it is a straightforward matter to obtain the fields inside region I and the scattered field by using equation (36) for  $r \in I$  and  $|\mathbf{r}'| > a$  respectively. Since for an arbitrary shape it is not expected that equation (36) can be solved exactly, an approximate technique must be used. A Galerkin procedure or a Born approximation can be applied.

Finally, it should be noted that for a circular inhomogeneity, as shown in figure 2, the field inside the inner cylinder (i.e.  $r_2 < b$ ) can be described by an expansion such as the one given in equation (4). From this expansion exactly the same results are obtained by solving the integral equation with those of § 2. This provides a valuable check on all previous formulae and results of the paper.

#### 4. Numerical computations

Numerical computations have been carried out for eccentric circular inhomogeneities. A computer program has been developed for the  $E$  and  $H$  incident wave cases. The coefficients  $A_m^{E,H}(0)$ ,  $A_m^{E,H}(1)$  and  $A_m^{E,H}(2)$  are computed by using equations (24), (25) and (26) where the convergence of the series is ensured by including in the summation terms of index  $|K - m|$  larger than  $t$ . Bessel and Neuman functions are computed by standard routines based on well known methods (Abramowitz and Stegun 1961). More specifically,  $|K - m|$  was extended up to  $2t$  and the convergence of the series was checked in each individual case numerically. In tables 1 and 2 results are given for the coefficients  $A_m^E(0)$ ,  $A_m^E(1)$  and  $A_m^E(2)$ , corresponding to small and large eccentricities (i.e.  $t$ ), respectively. It is shown that for  $t \ll 1$  only the dominant partial waves are

**Table 1.** Convergence of perturbation series coefficients for  $n = 1.3$ ,  $a = 5.0$ ,  $b = 0.3$ ,  $d = 0.3$ ,  $k = 1.0$ ,  $\phi_0 = 0.0$ .

$m$	$A_{Im}^E(0) = (-1)^m A_{1-m}^E(0)$	$A_{Im}^E(1) = (-1)^m A_{1-m}^E(1)$	$A_{Im}^E(2) = (-1)^m A_{1-m}^E(2)$
0	1.96(-1) + i1.02(0)	-5.00(-1) + i4.59(-1)	-8.82(-1) + i8.11(-1)
1	-9.22(-1) - i1.69(-2)	1.01(-1) - i3.74(-2)	1.78(-1) - i6.34(-2)
2	-2.77(-1) - i1.09(0)	-1.05(-2) + i1.14(-2)	-1.90(-2) + i1.94(-2)
3	8.03(-1) - i2.53(-1)	3.97(-4) - i4.02(-4)	7.27(-4) - i6.75(-4)
4	2.67(-1) + i1.01(0)	-4.22(-5) + i1.84(-5)	-7.56(-5) + i2.78(-5)
5	-6.15(-1) + i1.05(0)	6.22(-7) - i2.41(-6)	1.39(-6) - i4.11(-6)
6	-6.00(-1) - i4.17(-2)	4.81(-9) + i2.52(-8)	4.53(-9) + i4.43(-8)
7	2.69(-3) - i3.50(-1)	5.77(-10) + i1.35(-10)	9.69(-10) + i3.33(-10)



**Table 2.** Convergence of perturbation series coefficients for  $n = 1.3$ ,  $a = 5.0$ ,  $b = 0.3$ ,  $d = 4.0$ ,  $k = 1.0$ ,  $\phi_0 = 0.0$ .

$m$	$A_{1m}^E(0) = (-1)^m A_{1-m}^E(0)$	$A_{1m}^E(1) = (-1)^m A_{1-m}^E(1)$	$A_{1m}^E(2) = (-1)^m A_{1-m}^E(2)$
0	1.96(-1) - i1.02(0)	3.00(-2) + i5.48(-2)	5.41(-2) + i9.40(-2)
1	-9.22(-1) - i1.69(-2)	-2.48(-2) - i1.46(-1)	-4.26(-2) - i2.55(-1)
2	-2.77(-1) - i1.09(0)	1.38(-2) + i5.15(-3)	2.20(-2) + i1.12(-2)
3	8.03(-1) - i2.53(-1)	4.67(-2) + i1.06(-1)	8.21(-2) + i1.84(-1)
4	2.67(-1) + i1.01(0)	2.72(-3) - i2.32(-1)	5.97(-3) - i4.06(-1)
5	-6.15(-1) + i1.05(0)	1.70(-1) + i1.54(-1)	2.96(-1) + i2.71(-1)
6	-6.00(-1) - i4.17(-2)	3.60(-2) - i1.35(-1)	-6.29(-2) - i2.42(-2)
7	2.69(-3) - i3.50(-1)	-1.01(-2) + i9.03(-3)	-1.80(-2) + i1.56(-2)

distorted whereas for  $kd \sim ka$  (i.e.  $y \approx t$ ) a spread to all of the partial waves occurs. Note that the convergence of the perturbation series is determined from the value of  $x' - x = (n' - n)k_0b$ , i.e. the additional phase-shift inside the inhomogeneous region. The convergence of the series in equation (28), for the scattered field, is determined from the size of  $nk_0a = y$ . As in ordinary scattering (by homogeneous circular cylinders) the number of terms which must be summed is slightly larger than  $y = nk_0a$ . For  $H$ -wave polarisation a similar behaviour is observed. In figures 3 and 4 scattering patterns for a specific scatterer are given. Note that, even for a small value of  $k_0b(n' - n)$ , the asymmetry of the side lobes is detectable. It should also be noted that within the restriction  $|x' - x| < 1$  the method can be used for any values of  $k_0a$ ,  $k_0d$  and  $n$ . This is an advantage over certain numerical methods, such as the method of moments, where the matrix size could be a restrictive factor for the case of large  $k_0a$ ,  $k_0d$  and  $n$  values. Finally, in table 3, and for several incident wave directions, the total ( $\sigma_T$ ) and backscattering ( $\sigma_B$ ) cross sections are evaluated for a specific scatterer. It can be seen that  $\sigma_B$  undergoes an almost 60% change or a  $0^\circ$  to  $90^\circ$  change in the direction of incidence. This is an indication of the existing inhomogeneities.

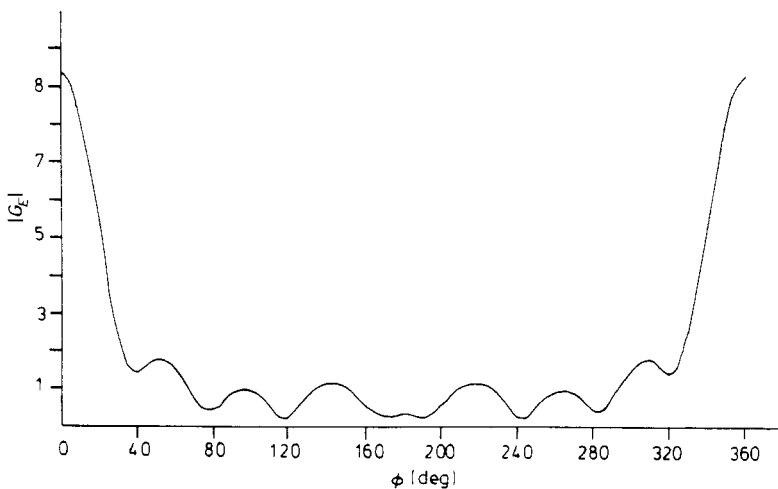


**Figure 3.** Scattering intensity  $|G^E(\phi)|$  as a function of  $\phi$  for an eccentric circular inhomogeneous cylindrical scatterer,  $k_0 = 1.0$ ,  $d = 4.0$ ,  $n' = 2.0$ ,  $n = 1.3$ ,  $a = 5.0$ ,  $b = 0.3$  and  $\phi_0 = 0.0$ .

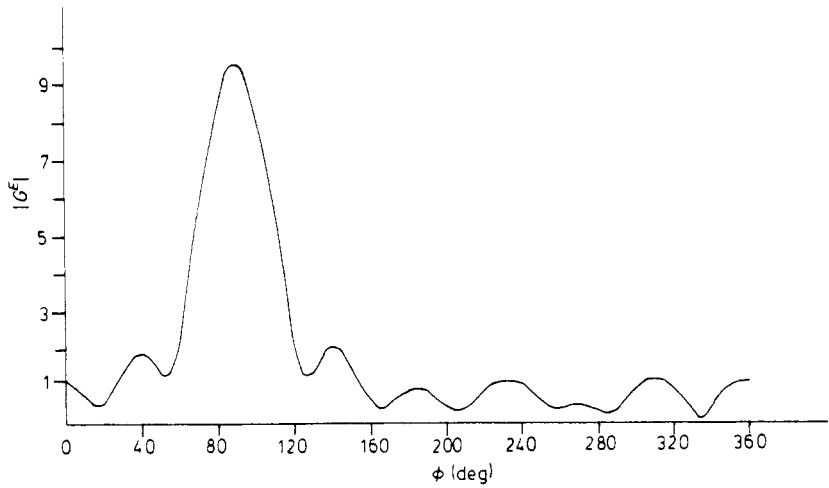


Figure 4. The same scatterer of figure 3 with  $\phi_0 = \frac{1}{2}\pi$ .

Table 3. Total ( $\sigma_T$ ) and backscattering ( $\sigma_B$ ) cross sections for  $k = 1.0$ ,  $a = 5.0$ ,  $b = 0.3$ ,  $n' = 2.0$ ,  $n = 1.3$ ,  $d = 4.0$  and several incident waves.

$\phi_0$	Polarisation	$\sigma_T$	$\sigma_B$
0°	<i>H</i>	3.44	1.56
90°	<i>H</i>	3.46	1.40
0°	<i>E</i>	3.58	1.26
90°	<i>E</i>	3.66	2.00

### 5. Conclusions

The problem of scattering from arbitrarily shaped inhomogeneous cylindrical scatterers is investigated. For eccentric circular inhomogeneities embedded in a circular cylinder a perturbation technique is developed. The perturbation series expansion parameter is proportional to the index of refraction difference between the outer and inner cylinders. The method is very powerful from the computational viewpoint. For a general, arbitrary inhomogeneity a Green function approach is developed which can be easily applied in conjunction with numerical or perturbation techniques. Numerical computations show that valuable information can be obtained about the inner structure of a body by observing the field scattered from it.

### Appendix 1. Proof of the cylindrical translational theorem

According to Stratton (1941, p 374) and the related figure in the same reference we have

$$H_n^{(1)}(\lambda r_1) \exp(in\psi) = \sum_{m=-\infty}^{+\infty} J_m(\lambda r_0) H_{n+m}^{(1)}(\lambda r) \exp[im(\theta - \theta_0)]$$

for  $|r| > |r_0 \cos(\theta - \theta_0)|$ , where  $\psi = \theta_1 - \theta$ . Since we always use  $\theta_0 = 0$  we have

$$\begin{aligned}
 H_n^{(1)}(\lambda r_1) \exp(in\theta_1) &= \sum_{m=-\infty}^{+\infty} J_m(\lambda r_0) H_{n+m}^{(1)}(\lambda r) \exp[i(m+n)\theta] \\
 &= \sum_{K=-\infty}^{+\infty} J_{K-n}(\lambda r_0) H_K^{(1)}(\lambda r) \exp(iK\theta)
 \end{aligned}$$

where we have redefined the summation index. The last expression is exactly the same as our equation (9).

**Appendix 2. Expansion coefficients for  $F_m^{E,H}(x', x)$**

The perturbation coefficients of equation (22) are obtained by evaluating (7) and (8). Following some very lengthy algebra and using the recurrence relations for Bessel functions we obtain

$$\begin{aligned}
 F_m^E(1) &= \frac{1}{2}\pi[2mJ_m(x)J_{m+1}(x) - x(J_{m+1}^2(x) + J_m^2(x))] \\
 F_m^E(2) &= \frac{1}{2}\pi[J_{m+1}^2(x) - J_m^2(x) - 2(m/x)J_m(x)J_{m+1}(x)] \\
 &\quad - \frac{1}{4}\pi^2[x(Y_{m+1}J_{m+1}(x) + Y_m(x)J_m(x))] \\
 &\quad - m(Y_{m+1}(x)J_m(x) + Y_m(x)J_{m+1}(x)) \\
 &\quad \times [2mJ_m(x)J_{m+1}(x) - x(J_{m+1}^2(x) + J_m^2(x))] \\
 F_m^H(1) &= -\frac{1}{2}\pi\{J_m^2(x)[x + (2m/x)] - 2(m+1)J_m(x)J_{m+1}(x) + xJ_{m+1}^2(x)\} \\
 F_m^H(2) &= \frac{1}{2}\pi[(m-1)2J_m(x)J_{m+1}(x)x^{-1} + J_m^2(x) - J_{m+1}^2(x) - (2m-1)(2m/x)J_m^2(x)] \\
 &\quad + \frac{1}{4}\pi^2[J_m^2(x)[x + (2m/x)] - 2(m+1)J_m(x)J_{m+1}(x) + xJ_{m+1}^2(x)] \\
 &\quad \times \{[(2m/x) + x]J_m(x)Y_m(x) + xJ_{m+1}(x)Y_{m+1}(x) - m + 1\}(Y_{m+1}(x)J_m(x) \\
 &\quad + Y_m(x)J_{m+1}(x)).
 \end{aligned}$$

**References**

Abramowitz M and Stegun I A 1972 *Handbook of Mathematical Functions* (New York: Dover)  
 Guru B S and Chen K M 1976 *IEEE MTT* **24** 433  
 Harrington R F 1968 *Field Computation by Moment Methods* (New York: Macmillan)  
 Kerker M 1969 *The Scattering of Light* (New York: Academic)  
 Latimer P and Pyle B E 1972 *Biophys. J.* **12** 764  
 Mittra R 1973 *Computer Techniques for Electromagnetics* (New York: Pergamon)  
 Mittra R and Lee S W 1971 *Analytical Techniques in the Theory of Guided Waves* (New York: Macmillan)  
 Morse P M and Feshbach H 1953 *Methods of Theoretical Physics part II* (New York: McGraw-Hill)  
 Sommerfeld A 1964 *Partial Differential Equations in Physics* (New York: Academic)  
 Stratton J A 1941 *Electromagnetic Theory* (New York: McGraw-Hill)  
 Wyatt P J and Phillips D T 1972 *J. Theor. Biol.* **37** 493